DEUTSCHES ELEKTRONEN-SYNCHROTRON DESY

DESY 81-075
November 1981

RECENT RESULTS FROM PETRA ON R, ON HADRONIC FINAL STATES AND ON INCLUSIVE HADRON SPECTRA

by

R. Felst

NOTKESTRASSE 85 · 2 HAMBURG 52

DESY 81-075
November 1981

RECENT RESULTS FROM PETRA ON R, ON HADRONIC FINAL STATES AND ON INCLUSIVE HADRON SPECTRA

R. FELST

DEUTSCHES ELEKTRONEN-SYNCHROTRON
DESY
HAMBURG, GERMANY

I. INTRODUCTION

It is now nearly three years since the first e^+e^- collisions were observed at PETRA, which opened a new energy range for experimental investigation. In the meantime a total luminosity of about 30 pb^{-1} has been accumulated in each of the four interaction regions at center-of-mass energies between 12 and 36.8 GeV (Fig. 1), and important new insights into the production of hadrons by e^+e^- - annihilation have been obtained by the experiments CELLO, JADE, MARK J, PLUTO and TASSO.

In the following recent results from these experiments concerning the gross features of the hadronic final state produced by e^+e^--annihilation are reported:

a) the total cross section for hadron production

b) the energy fractions of charged and neutral hadrons

c) the charged hadron multiplicities

d) inclusive hadron spectra.

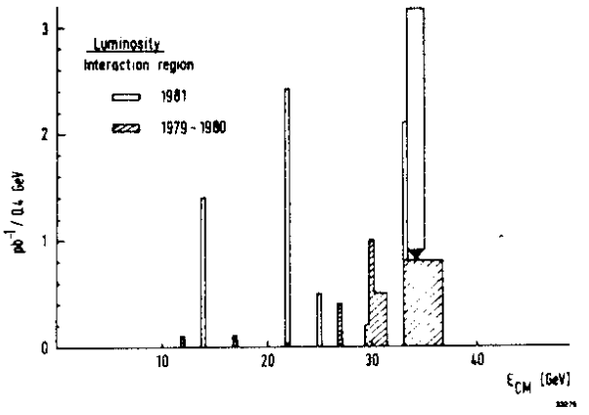

Fig. 1: Luminosity per interaction region accumulated at PETRA as a function of the center-of-mass energy.

Invited talk presented at the '1981 International Symposium on Lepton and Photon Interactions at High Energies' in Bonn, August 1981.

II. σ_{tot} (e^+e^- → hadrons)

Hadron production by e^+e^--annihilation is generally attributed to the diagram shown in Fig. 2a), and the measured data are corrected for higher order electromagnetic processes including hadronic vacuum polarisation[1]. The process is identified by the momentum balance of the final state particles and the well defined center-of-mass energy.

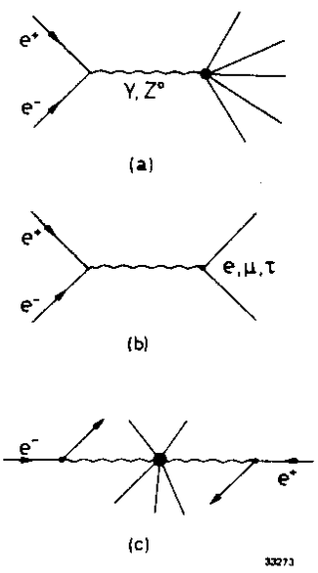

Fig. 2: First order diagram for hadron production by e^+e^--annihilation (a) and lepton pair production (b); (c) shows the diagram for hadron production by two-photon collisions.

The main background processes are the production of lepton pairs (Fig. 2b), which at PETRA energies are easy to identify and to reject, and the production of hadrons by the collision of two almost real photons (Fig. 2c). The hadronic system produced by $\gamma\gamma$-collision is in general of low mass and has a large momentum along the beam direction, which allows for discrimination from annihilation events. For details we refer to refs. 2.

One is of course aiming for a precise measurement of a quantity of such fundamental importance as σ_{tot}. At present the PETRA experiments quote systematic uncertainties ranging from ±5% (PLUTO) to ±10% (MARK J). The main sources of these uncertainties are in the measurement of the luminosity and in the precise knowledge of the acceptance of the apparatus and of the radiative corrections.

Fig. 3 shows the recent results on $R = \sigma_{tot}/\sigma_{\mu\mu}$ ($\sigma_{\mu\mu} = \frac{4\pi\alpha^2}{3s}$) from PETRA and some representative data at lower energies. In the energy ranges 29.9 - 31.6 GeV and 33.0 - 36.6 GeV data have been taken in a scanning mode, in order to search for narrow resonances. Since no evidence for such resonances has been found[3], we show in Fig. 3 the results averaged over larger energy intervals. The data of the five PETRA experiments agree well within the quoted systematic uncertainties (the errors shown in Fig. 3 are statistical only) and are consistent with a constant value of R.

The simple quark-parton-model prediction

$$R_0 = 3 \sum_f Q_f^2 = \frac{11}{3} \qquad (1)$$

(f runs over the quark flavours u, d, s, c, b with electric charges Q_f), which is also shown in Fig. 3, describes the high energy data reasonably well. This fact constitutes clear evidence for the colour degree of freedom and for the pointlike structure of quarks. Introducing a quark form factor F which modifies (1) $\quad R = R_0 \cdot F^2 \qquad (2)$

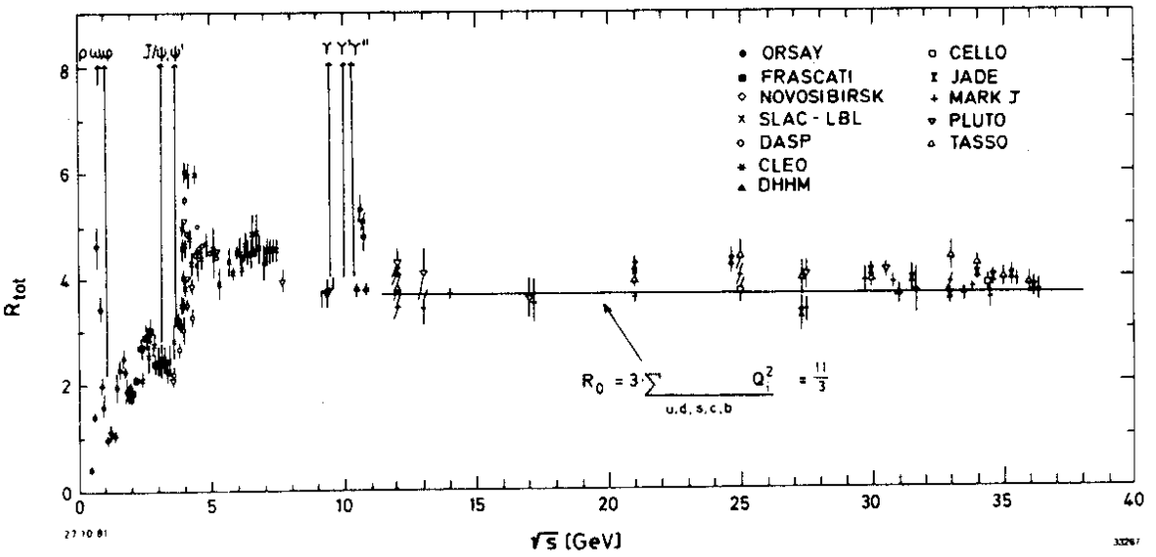

Fig. 3: Compilation of R values from the different PETRA experiments together with data from lower energies. Only statistical errors are shown. The quark-parton model prediction is also indicated.

Wolf and Söding[4] (using last year's data) and the MARK J group (using all their data) obtained upper limits for a possible quark substructure as listed in Table 1.

F	95% CL limit in (GeV)	author
$(1 - \frac{s}{M^2})^{-1}$	$M > 124$	ref. 4
$(1 - \frac{s}{M^2})^{-2}$	$M > 176$	ref. 4
$(1 \mp \frac{s}{s - \Lambda_\pm^2})$	$\Lambda_+ > 185$ $\Lambda_- > 280$	MARK J

TABLE 1

Upper limits for possible spatial structure of quarks, obtained from comparison with the quark parton model prediction for R.

The quark parton model predictions are refined by QCD in leading order to[5)]

$$R = R_0 \left(1 + \frac{\alpha_s}{\pi}\right)$$
$$\alpha_s = \frac{12\pi}{(33-2N_f) \cdot \ln(s/\Lambda^2_{QCD})} \qquad (3)$$

with N_f being the number of active flavours and Λ_{QCD} the scale parameter of QCD. Second order QCD corrections to R were found to be small[6)] and eq. (3) allows in principle a clear determination of α_s. However the QCD correction term is small and the effects of the weak neutral current are expected to be of similar size at the highest PETRA energies.

Including the neutral weak current in the standard way, one obtains the following modification of the quark parton model prediction[7)]:

$$R_0 \rightarrow 3 \sum_f R_f$$
$$R_f = Q_f^2 - \frac{2 s \rho Q_f v_e v_f}{\left(\frac{s}{M_Z^2} - 1\right) + \frac{\Gamma_Z^2}{s-M_Z^2}} \qquad (4)$$
$$+ \frac{s^2\rho^2 (v_e^2 + a_e^2)(v_f^2 + a_f^2)}{\left(\frac{s}{M_Z^2} - 1\right)^2 + \frac{\Gamma_Z^2}{M_Z^2}}$$

with M_Z and Γ_Z being the mass and the width of the Z^0 and a and v its axial and vector coupling constants, and $\rho = G_F/(8\sqrt{2}\cdot\pi\cdot\alpha)$. First order QCD corrections for eq. (4) have been calculated for heavy quarks by Jersak et al[8)]. The result of their calculation for $\Lambda_{QCD} = 0.3$ GeV and different values of $\sin^2\theta_w$ is shown in Fig. 4.

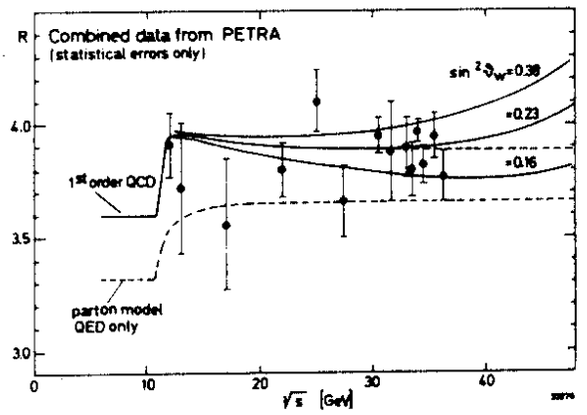

Fig. 4: The PETRA data of Fig. 3 averaged over the different experiments, considering statistical errors only. The full curves are the first order QCD predictions of Jersak et al. for $\Lambda_{QCD} = 0.3$ GeV and values of $\sin^2\theta_w$ as indicated. The broken curves represent the predictions without neutral weak currents.

Apart from the general increase of R (eq. (3)), the QCD corrections yield a considerable enhancement of R close above the threshold for b-quark production. Also shown in Fig. 4 are the experimental data from PETRA averaged over the different experiments. The averaging procedure, however, is questionable, since systematic uncertainties have been ignored.

The curves and data of Fig. 4 enable one, in principle, to determine two fundamental parameters, Λ_{QCD} and $\sin^2\theta_w$. At present, however, the accuracy of the data is not sufficient to measure both numbers independently. Considering only the data for $\sqrt{s} \geq 20$ GeV and assuming $\sin^2\theta_w = 0.23$ and an energy independent α_s we obtain values of α_s as listed in table 2. The error of α_s depends strongly on the normalization uncertainty, which remains after averaging the data. A ± 4% remaining uncertainty is probably a realistic number. Also listed in table 2 are similar results from the PLUTO and TASSO groups based on their data only. These values are in accord with the numbers obtained from lepton nucleon scattering, but one has to aim for systematic uncertainties in R of the order of 2% in order to obtain a significant measurement of α_s.

The determination of $\sin^2\theta_w$ from R yields two solutions. Taking the one which agrees with the lepton data we obtain from the data of Fig. 4, assuming $\Lambda_{QCD} = 0.1$ GeV and 4% normalization uncertainty, the results listed in Table 3. Also shown there are results from the JADE[9] and MARK J[10] groups. These values of $\sin^2\theta_w$ agree well with those obtained from low Q^2 processes involving light quarks only, whereas at PETRA energies c- and b-quarks contribute more than 40% to σ_{tot}.

data	normalization uncertainty	α_s	C.L.
all	± 4%	0.15 ± 0.15 ≤ 0.4	68% 95%
all	± 2%	0.16 ± 0.07 0.16 ± 0.15	68% 95%
PLUTO	0.30 ± 0.06 (stat.) ± 0.14 (system.)		
TASSO	0.30 ± 0.04 (stat.) ± 0.22 (system.)		

TABLE 2

Values of α_s deduced from the measurement of R assuming $\sin^2\theta_w = 0.23$, except for the PLUTO value, which was obtained ignoring the weak contribution. Errors corresponding to 68% and 95% confidence levels are given.

data	$\sin^2\theta_W$	C.L.
all	$0.24^{+0.06}_{-0.05}$	68%
	$0.24^{+0.36}_{-0.08}$	95%
JADE	$0.22^{+0.11}_{-0.09}$	68%
MARK J	$0.27^{+0.34}_{-0.08}$	68%
	$0.27^{+0.39}_{-0.12}$	95%

TABLE 3

Values of $\sin^2\theta_W$ deduced from the measurements of R assuming Λ_{QCD} = 0.1 GeV and 4% normalization uncertainty.

III. NEUTRAL ENERGY FRACTION

Further information about the gross features of the hadronic final state is provided by a measurement of the fraction of the energy carried by gamma rays and by all neutral particles.

The gamma ray energy fraction ρ_γ has been obtained by the CELLO and JADE groups from measurements of the energy deposited in a photon detector surrounding the interaction region, whereas the neutral energy fraction ρ_N has been determined by the JADE-group as the complement of the charged energy fraction $\rho_N = 1 - \rho_{charged}$. The resulting values of ρ_γ and ρ_N for the multihadron events, i.e. those events passing the selection criteria of the σ_{tot} $(e^+e^- \to \text{hadrons})$ measurement, are shown in Fig. 5.

Both fractions ρ_γ and ρ_N are independent, within the experimental errors, of the center-of-mass energy. Similar values of ρ_N have been obtained by the Crystal Ball experiment at SPEAR[12], which indicates practically constant fractions ρ_N from the charm threshold up to 35 GeV.

The difference $\rho_N - \rho_\gamma$ provides an upper limit on the amount of energy carried by neutrinos. The JADE-group obtains a 95% C.L. upper limit of about 10% on the fraction of energy carried away by neutrinos. This upper limit strongly disfavours the Pati-Salam model[13] with free integer charged quarks, which predicts a neutrino energy fraction between 18% and 28%. The observed number is however in accord with models based on perturbative QCD including standard quark and gluon fragmentation[14].

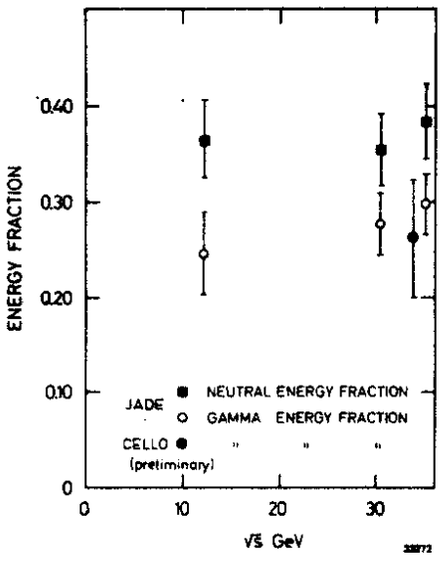

Fig. 5: Mean gamma ray and neutral energy fractions versus center-of-mass energy.

IV. CHARGED HADRON MULTIPLICITIES

More details of hadronic final state and its production mechanism are revealed by the hadron multiplicity distribution $\langle N_{ch} \rangle$. The mean multiplicity of charged particles, including particles from K^0_S decays, is plotted in Fig. 6. Data from a recent more refined evaluation by JADE are shown together with published data from PLUTO[15] and TASSO[16] and from measurements at lower energies[17].

The PETRA data of $\langle N_{ch} \rangle$ rise faster with increasing energy than expected from an extrapolation linear in ln s of the low energy data, as expected from Feynman scaling[18]. Models based on first order perturbative QCD, however, with subsequent fragmentation of quarks and gluons into hadrons according to the prescription of Field and Feynman[14], describe the data above 10 GeV rather well, as indicated in Fig. 6. The inclusion of gluon bremsstrahlung alters the $q\bar{q}$ prediction only slightly. One might, therefore, argue that there is only at $\sqrt{s} \approx 10$ GeV enough energy available for the full cascade mechanism to develop. Next-to-leading-order QCD calculations[19] indicate a parton multiplicity rising at very high energies according to $\langle N_{parton} \rangle \sim \exp(1.77\sqrt{\ln(s/\Lambda^2)})$. Fitting the data of Fig. 6 with an expression of the form $\langle N_{ch} \rangle = N_o + a \cdot \exp(b \cdot \sqrt{\ln(s/\Lambda^2)})$ we obtain for $\Lambda = 0.3$ GeV (curve A in Fig. 6) the parameters $N_o = 2.0 \pm 0.2$, $a = 0.027 \pm 0.01$, $b = 1.9 \pm 0.2$. Also the simple dependence $\langle N_{ch} \rangle \sim s^{1/4}$ (curve B in Fig. 6), predicted by the statistical model of Fermi[20] for hadron collisions and by some hydrodynamical models[21] for e^+e^--annihilation, reproduces the data rather well.

The simple statistical model, however, does not describe the dispersion $D_{ch} = \sqrt{\langle N^2_{ch} \rangle - \langle N_{ch} \rangle^2}$ of multiplicities, which was found to increase like $\langle N_{ch} \rangle$.
The ratio $\langle N_{ch} \rangle / D_{ch}$ plotted in Fig. 7 shows within the experimental errors no significant energy dependence and does not follow $\sqrt{\langle N_{ch} \rangle}$, which would be predicted for a Poisson-like distribution.

The charged particle multiplicity distribution is shown in Fig. 8 on an KNO-plot[22] in which $\langle N_{ch} \rangle \cdot P_{N_{ch}}$ is plotted versus $N_{ch}/\langle N_{ch} \rangle$, where $P_{N_{ch}}$ is the probability of observing the charged multiplicity N_{ch}. The multiplicity distribution at different energies coincides within errors and has a shape similar to the one observed in $p\bar{p}$ annihilation[23].

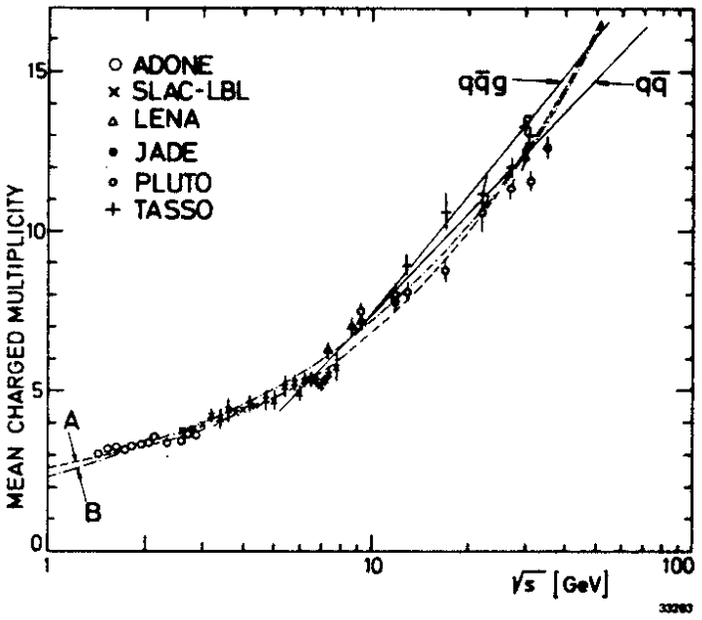

Fig. 6: Mean charged multiplicity versus center-of-mass energy. The straight line labelled $q\bar{q}$ is a typical prediction for $q\bar{q}$ production with subsequent fragmentation of quarks into mesons. The line labelled $q\bar{q}g$ includes gluon bremsstrahlung. The curve labelled (A) is the best fit of the form $\langle N_{ch}\rangle = N_o + a \cdot \exp(b\sqrt{\ln(s/\Lambda^2)})$ described in the text. Curve (B) shows the dependence $\langle N_{ch}\rangle = 2.3 \cdot s^{1/4}$ (s in GeV^2).

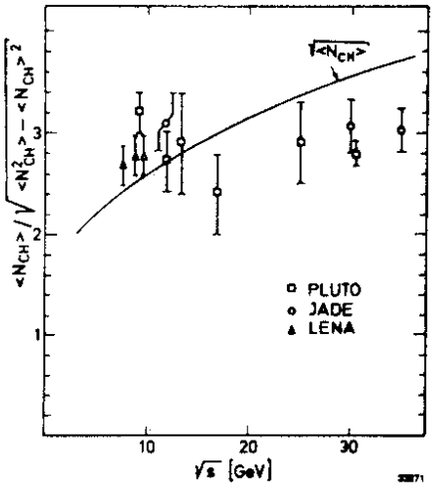

Fig. 7: Energy dependence of the ratio $\langle N_{ch}\rangle / D_{ch}$.

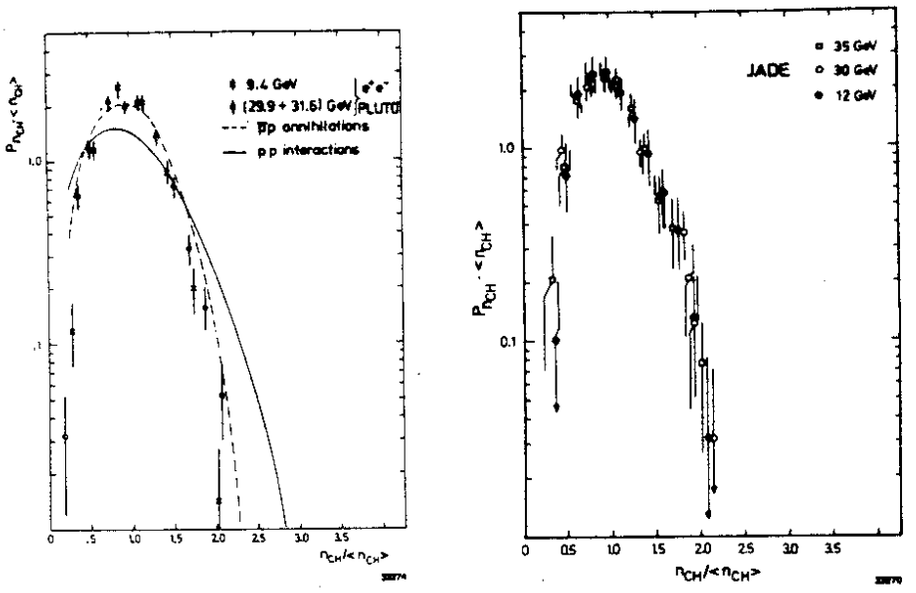

Fig. 8: KNO plot of the PLUTO and JADE data. $P_{N_{ch}}$ is the probability of observing the charged multiplicity N_{ch}.

V. INCLUSIVE HADRON SPECTRA

Charged particle momentum spectra have recently been measured with increased precision and mesons ($\pi^{\pm}$, π^0 and K^S_0) as well as baryons (Λ-particles) have been identified over a large momentum range. Charged particle inclusive momentum distributions $s \cdot \frac{d\sigma}{dx_p}$, $x_p = p/p_{beam}$, are shown in Fig. 9. The data of the CELLO, JADE, and TASSO experiment are in reasonable agreement and satisfy within about 20% the relation

$$\frac{1}{\sigma_{\mu\mu}} \int \frac{d\sigma}{dx_p} dx_p = \frac{3}{4\pi\alpha^2} \int s \frac{d\sigma}{dx_p} dx_p = R \cdot \langle N_{ch} \rangle . \qquad (5)$$

The cross section $s \frac{d\sigma}{dx_p}$ rises at small x strongly with increasing center-of-mass energy, and is for the PETRA experiments for $x_p \gtrsim 0.2$ independent of s to within about 50%. Significant scaling violations at large x are only visible in comparison to the SLAC-LBL[24] data measured at 7.4 GeV which are also shown in Fig. 9, together with the data from the DASP[25] group measured at 5.0 GeV.

Charged pions have been identified by the TASSO group within essentially the full momentum range using time-of-flight measurement and Cerenkov counter techniques and within a limited momentum range by the JADE group by means of dE/dx measurements. Neutral pions were measured by the TASSO group using a lead-liquid-Argon calorimeter. The results are plotted in Fig. 10 in form of the scaling

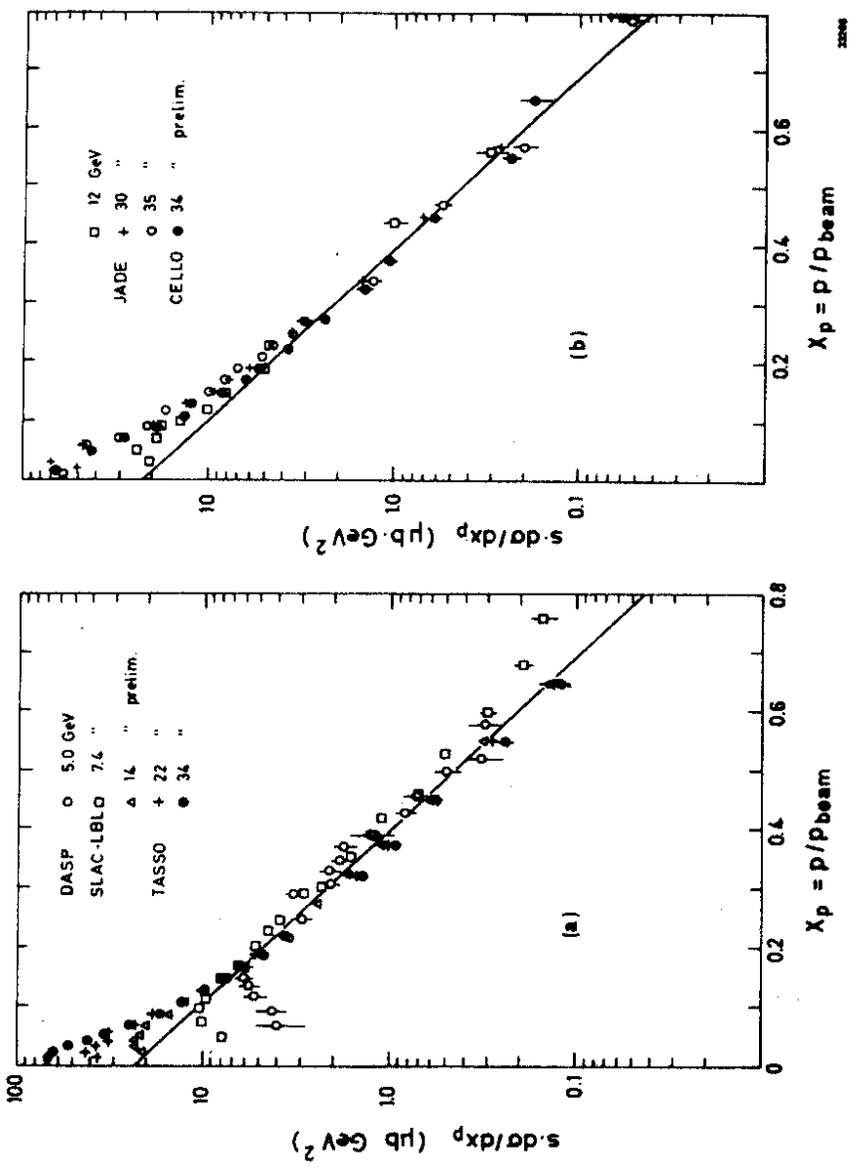

Fig. 9: Inclusive spectrum $s \cdot d\sigma/dx_p$ of charged particles. (a) shows the data of the TASSO group together with results from the SLAC-LBL and DASP groups at lower energies. (b) shows the data from the CELLO- and JADE group. The full lines are drawn to guide the eye and correspond to $s \cdot d\sigma/dx_p = 23 \cdot \exp(-8 \cdot x_p)$ μb GeV^2.

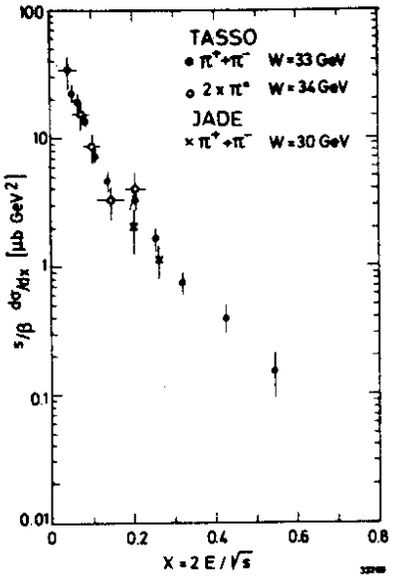

Fig. 10: The cross section $s/\beta\ d\sigma/dx$ for charged and neutral pion production versus x.

cross section $s/\beta\ d\sigma/dx$, $x = 2E/\sqrt{s}$.

Neutral kaons have been identified by kinematical reconstruction of $K^0_S \to \pi^+\pi^-$ decays by the JADE, PLUTO[26], and TASSO[27,29] group. The resulting scaling cross sections are shown in Fig. 11.

Also Λ particles have recently been identified by kinematical reconstruction. JADE[28] using the $\bar{\Lambda} \to \bar{p}\pi^+$ channel identifies the $\bar{p}$ and π^+ by dE/dx, and obtains a clear $\bar{\Lambda}$ signal. The momentum range is limited to $p_{\bar{\Lambda}} \leq 1.4$ GeV/c. This is not the case for the TASSO[29] results, which are based on Λ and $\bar{\Lambda}$ identification by kinematical reconstruction only. Fig. 12a shows the Λ momentum spectrum $d\sigma/dp$ together with the proton spectrum[28,30], which covers however only the low momentum region. For momenta around 1 GeV/c the

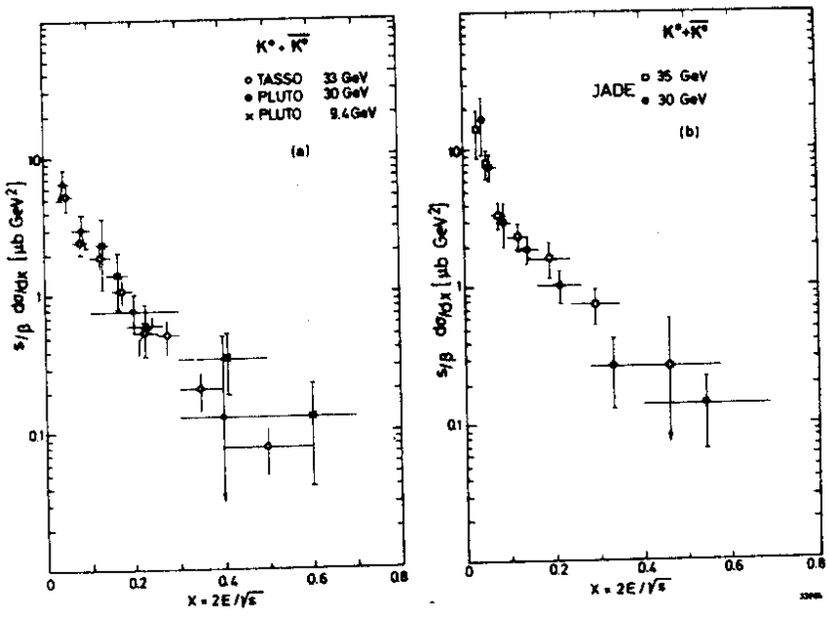

Fig. 11: The cross section $s/\beta\ d\sigma/dx$ for neutral kaons versus x. (a) shows the data from PLUTO and TASSO and (b) the data from JADE.

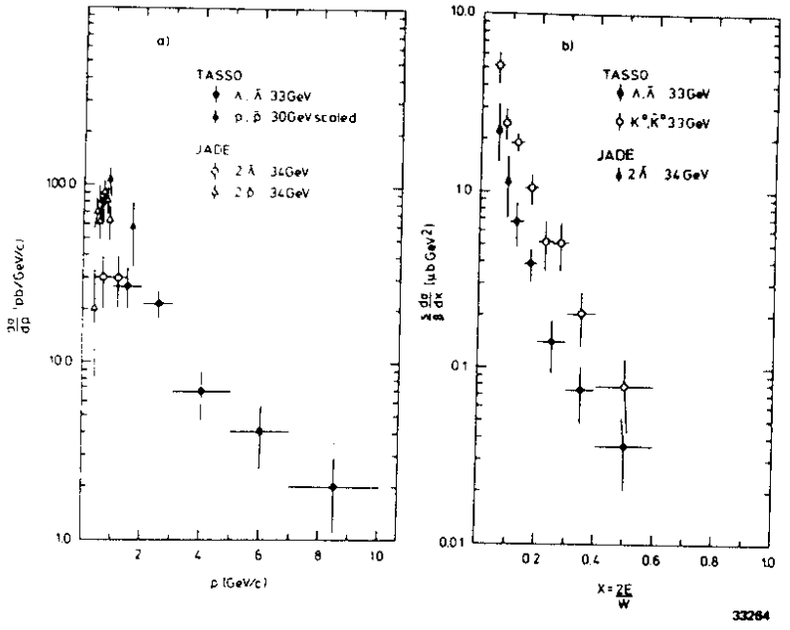

Fig. 12: Proton and lambda momentum spectra dσ/dp versus p are shown in (a) and the cross section s/β dσ/dx for lambda particles in (b).

Λ cross section dσ/dp amounts to about 1/3 of the proton cross section. Fig. 12b shows the scaling cross section for Λ production.

It is striking that the scaling cross sections for π, K and Λ production have roughly the same shape for x ≳ 0.2. This is demonstrated in Fig. 13 where the TASSO π, K and Λ data are plotted together. It might seem somewhat surprising that the x-dependence for baryon production is similar to

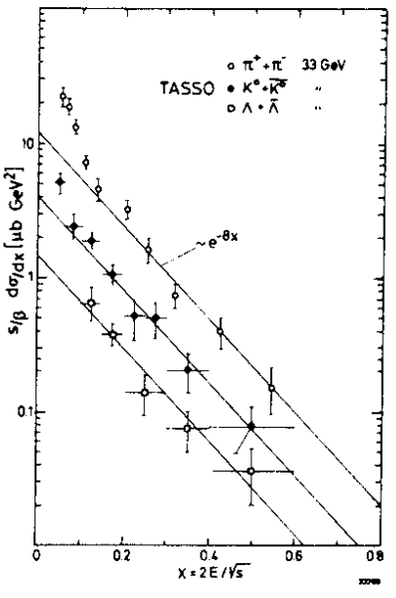

Fig. 13: Scaling cross sections s·dσ/dx together for π, K and Λ production. The lines, which are only drawn to guide the eye, represent curves ∼ exp (-8·x).

the one for mesons. Models[31], however, which treat diquark pairs similarly to quark pairs in the fragmentation cascade process are able to reproduce this behaviour.

The baryon production rate seems also to be rather high. At 33 GeV one finds $\langle N_{ch} \rangle = 13 \pm 1$, $\langle N_{K^0+\bar{K}^0} \rangle = 1.5 \pm 0.3$ and $\langle N_{\Lambda+\bar{\Lambda}} \rangle = 0.28 \pm 0.06$. The Λ production alone amounts to about 20% of the K^0 production. Similar ratios

$\langle N_\Lambda \rangle / \langle N_{K^0} \rangle$ have been observed in $\pi^+ p$ [32] and νp [33] reactions.

VI. SUMMARY

The total cross section σ_{tot} ($e^+e^- \to$ hadrons) measured by the PETRA experiments CELLO, JADE, PLUTO, MARK J and TASSO shows 1/s dependence within the energy range covered, 144 GeV$^2 \leq s \leq$ 1340 GeV^2. Its size agrees to within about 10% with the parton model prediction for pointlike coloured quarks with flavours u, d, s, c, and b. There is evidence for the small QCD correction term but its clear confirmation needs measurements to an accuracy of about 2%. Weak neutral currents, even at the highest PETRA energies, do not contribute significantly to σ_{tot}, which implies within the framework of the standard model $\sin^2\theta_w = 0.24 \pm 0.06$.

The fraction of the total available energy carried by photons and the fraction carried by neutral particles of all types show no strong dependence on center-of-mass energy. The neutrino energy fraction is less than 10% at the 95% confidence level.

The charged particle multiplicity rises faster than expected from an extrapolation, linear in ln$s$, of the low energy data; the dispersion of the multiplicity is roughly proportional to $\langle N_{ch} \rangle$ and KNO-scaling holds within the errors.

The inclusive cross sections $s/\beta \frac{d\sigma}{dx}$ for π, K^0 and Λ production show roughly the same x-dependence for $x \gtrsim 0.2$. Baryon production is not negligible. The Λ production alone amounts to about 20% of the K^0 production.

Acknowledgements

I wish to thank the physicists of the PETRA experiments for the cooperation, Dr. E. Elsen for his help with the data and Mrs. S. Platz for the careful typing.

REFERENCES

1) F.A. Berends and R. Kleiss, Nucl. Phys. B186 (1981) 22 and references therein

2) CELLO Coll. H.-J. Behrend et al., DESY 81-029 (1981)
JADE Coll. W. Bartel et al., Phys. Lett. 88B (1979) 171
MARK J Coll. D. Barber et al., Phys. Rev. Lett. 43 (1979) 901
PLUTO Coll. Ch. Berger et al., Phys. Lett. 81B (1979) 410
TASSO Coll. R. Brandelik et al., Phys. Lett. 83B (1979) 261

3) for details see J. Bürger: "Recent Results from PETRA on Search for New Particles", these proceedings

4) P. Söding, G. Wolf, DESY 81-13, to be published in "Annual Review of Nuclear and Particle Science"

5) T. Applequist and H. Georgi, Phys. Rev. D12 (1975) 1404
E.C. Poggio et al., Phys. Rev. D13 (1976) 1958

6) M. Dine, J. Sapirstein, Phys. Rev. Lett. 43 (1979) 668
K.G. Chetyrkin et al., Phys. Lett. 85B (1979) 277
W. Celmaster, R.J. Gonsalves, Phys. Rev. Lett. 44 (1979) 560

7) J. Ellis and M.K. Gaillard, Physics with very high energy e^+e^- colliding beams, CERN 76-18; J. Ellis, Weak interactions at high energies, Proc. SLAC Summer Institute (1978)

8) J. Jersak et al., Phys. Lett. 98B (1981) 363

9) JADE Coll. W. Bartel et al., Phys. Lett. 101B (1981) 361

10) MARK J Coll. D. Barber et al., Phys. Rev. Lett. 46 (1981) 1663

11) JADE Coll. W. Bartel et al., Z. Phys. C9 (1981) 315

12) E. Bloom, SLAC-PUB-2425 (1979) and Proceedings of the 1979 International Symposium on Lepton and Photon Interactions at High Energies, Fermilab, August 1979, 92

13) J.C. Pati and A. Salam, Nucl. Phys. B144 (1978) 445

14) see for details the talk by D. Fournier in these proceedings

15) PLUTO Coll. Ch. Berger et al., Phys. Lett. 95B (1980) 313

16) TASSO Coll. R. Brandelik et al., Phys. Lett. 89B (1980) 418

17) C. Bacci et al., Phys. Lett. 86B (1979) 234;
LENA Coll. B. Niczyprouk et al., DESY 81-008;
J.L. Siegrist, SLAC-225, (1979)

18) R.P. Feynman, Phys. Rev. Lett. 23 (1969) 1415

19) A.H. Mueller, CU-TP 197, Columbia University, 1981

20) E. Fermi, Prog. Theor. Phys. 5 (1950) 570

21) T.F. Hoang and Bruce Cork LBL-11806 preprint (1980)

22) Z. Koba, H.B. Nielson and P. Olesen, Nucl. Phys. B40 (1972) 317

23) J. Salava and V. Simak, Nucl. Phys. B40 (1972) 317

24) J.L. Siegrist, SLAC-225 (1979)

25) DASP-Coll. R. Brandelik et al., Nucl. Phys. B148 (1979) 189

26) PLUTO Coll. Ch. Berger et al., Phys. Lett. 104B (1981) 79

27) TASSO Coll. R. Brandelik et al., Phys. Lett. 94B (1980) 91

28) JADE Coll. W. Bartel et al., Phys. Lett. 104B (1981) 325

29) TASSO Coll. R. Brandelik et al., Phys. Lett. 105B (1981) 75

30) TASSO Coll. R. Brandelik et al., Phys. Lett. 94B (1981) 444

31) B. Andersson et al., LU TP 81-3, Lund University, preprint (1981); Th. Meyer, DESY 81-046 (1981)

32) P. Bosetti et al., Aachen-Bonn-CERN-Cracow Coll., Nucl. Phys. B94 (1975) 21

33) H. Grässler et al., Aachen-Bonn-CERN-Munich-Oxford Coll. , CERN/EP 81-56